On-the-fly semiclassical study of internal conversion rates of Formaldehyde

Reuven Ianconescu

Shenkar College of Engineering and Design and Chemical Physics Department,
Weizmann Institute of Science, 76100 Rehovoth, Israel

Jörg Tatchen

Departamento de Química, Universidad de los Andes, Bogotá, Colombia

Eli Pollak[a]

Chemical Physics Department, Weizmann Institute of Science, 76100 Rehovoth, Israel

(Dated: August 11, 2018)

Abstract

Internal conversion is an inherently quantum mechanical process. To date, "ab-initio" computation of internal conversion rates was limited to harmonic based approximations. These are questionable since the typical transition to the ground electronic state occurs at energies which are far from the harmonic limit. It is thus of interest to study the applicability of the Semiclassical Initial Value Representation (SCIVR) approach which is in principle amenable to "on the fly" studies even with "many" degrees of freedom. In this work we apply the Herman-Kluk-SCIVR methodology to compute the internal conversion rates for Formaldehyde for a variety of initial vibronic states. The SCIVR computation gives reasonable agreement with experiment, while the harmonic approximation typically gives rates that are too high.

[a] email: eli.pollak@weizmann.ac.il

PACS numbers:

I. INTRODUCTION

The Internal Conversion (IC) rate plays an important role in determining the lifetime of electronically excited states. It is of major interest in the design of light emitting molecules, since the light emitting efficiency is governed by the competition between radiative and radiationless decay processes [1].

The study of the nonradiative decay of excited vibronic states has a long history. Lin and Bersohn [2, 3] set the framework over forty years ago in their seminal papers. A summary of the historical development of the theory may be found in a recent review by Lin et al [4]. These studies are though limited to harmonic models for the vibrations in both the ground and excited electronic state [5]. At best, anharmonicity is dealt with using perturbation theory about the harmonic limit as described for example in Refs. [6–8].

Especially for IC, where the transition occurs from an excited electronic state to high energy vibrations in the ground electronic state, one may expect that the harmonic approximation for the dynamics and its extensions on the ground state potential may fail. The density of vibrational states on the ground electronic state is typically much higher than predicted from a harmonic model. In a previous model computation for a system with two degrees of freedom we demonstrated this failing of the harmonic based theories [9].

An important advantage of the harmonic theory is that one may use ab-initio methods for the force fields and thus estimate from first principles the IC rates [7, 8, 10, 11]. This is not the case when one attempts to use numerically exact quantum computations such as the MultiConfiguration Time Dependent Hartree (MCTDH) method [12]. Quantum mechanical propagation methods need to employ a global force field which is rather difficult to obtain for multidimensional systems. One approximate way of overcoming this difficulty is by using a reaction path Hamiltonian for classifying the degrees of freedom into small amplitude coordinates and large amplitude coordinates [13].

An alternative approach would be to use the Semiclassical Initial Value Representation (SCIVR) approach [14]. SCIVR is known to treat quantum effects such as zero point energy, superposition and weak to moderate tunneling rather well. Especially the Herman-Kluk (HK) frozen Gaussian SCIVR propagator [15] is amenable to ab-initio computations in the sense that it relies on the dynamics of the bare potential and needs as input only the local force field and its spatial derivative.

In previous work, we tested the HK SCIVR approximation on a model system with two coupled anharmonic degrees of freedom [9]. We found that the HK SCIVR is an excellent approximation to the exact quantum dynamics, while the harmonic approximation was unsatisfactory. The SCIVR has been used previously rather successfully within an ”on-the-fly” approach. Ceotto and coworkers have implemented various versions to study the dynamics of the water molecule [16] and Fermi splittings for CO_2 [17, 18]. The same group has also recently presented an on-the-fly study of the ground state dynamics of the Formaldehyde molecule [19]. A frozen Gaussian SCIVR has been also used successfully to compute an on-the-fly photo-absorption spectrum of Formaldehyde in Ref. [20].

In this paper we implement an on-the-fly application of the HK SCIVR approximation for the computation of internal conversion rates for Formaldehyde. The central objective of this paper is to compare results obtained with the HK-SCIVR method for vibronic internal conversion rates with experiment and a harmonic approximation. We find that the semiclassical theory gives reasonable agreement with the experiment and is quite superior to the harmonic based estimates.

The theoretical framework needed for implementation of the HK-SCIVR theory to internal conversion is given in Section II. The actual implementation and comparison with experiment and the harmonic results is described in Section III. We end with some concluding remarks in Sec. IV.

II. THEORETICAL FRAMEWORK

A. The electronic structure of Formaldehyde

The TURBOMOLE package [22] was used to compute the force field needed for Formaldehyde CH_2O as presented in this section. We used DFT with the b-p functional [29], and our basis functions were def2-TZVP [27]. Our SCF convergence criterion was 10^{-9}, and our grid was “m3” employing a coarser grid at the beginning of the SCF iterations, and grid of 3 in the final SCF iteration and the gradient evaluation [28].

The molecular shape of Formaldehyde is trigonal planar, the equilibrium positions in the ground electronic state are shown in Figure 1. The six normal modes of the molecule are described in Figure 2.

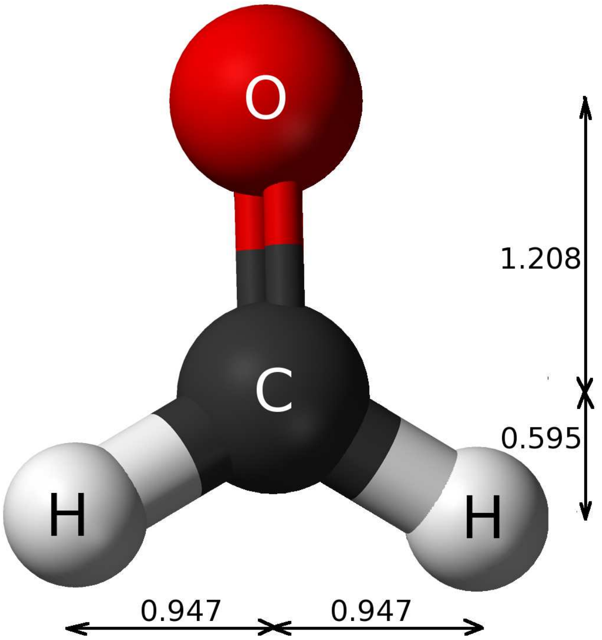

FIG. 1: The equilibrium structure of Formaldehyde in the ground electronic ground state. Lengths are given in Å.

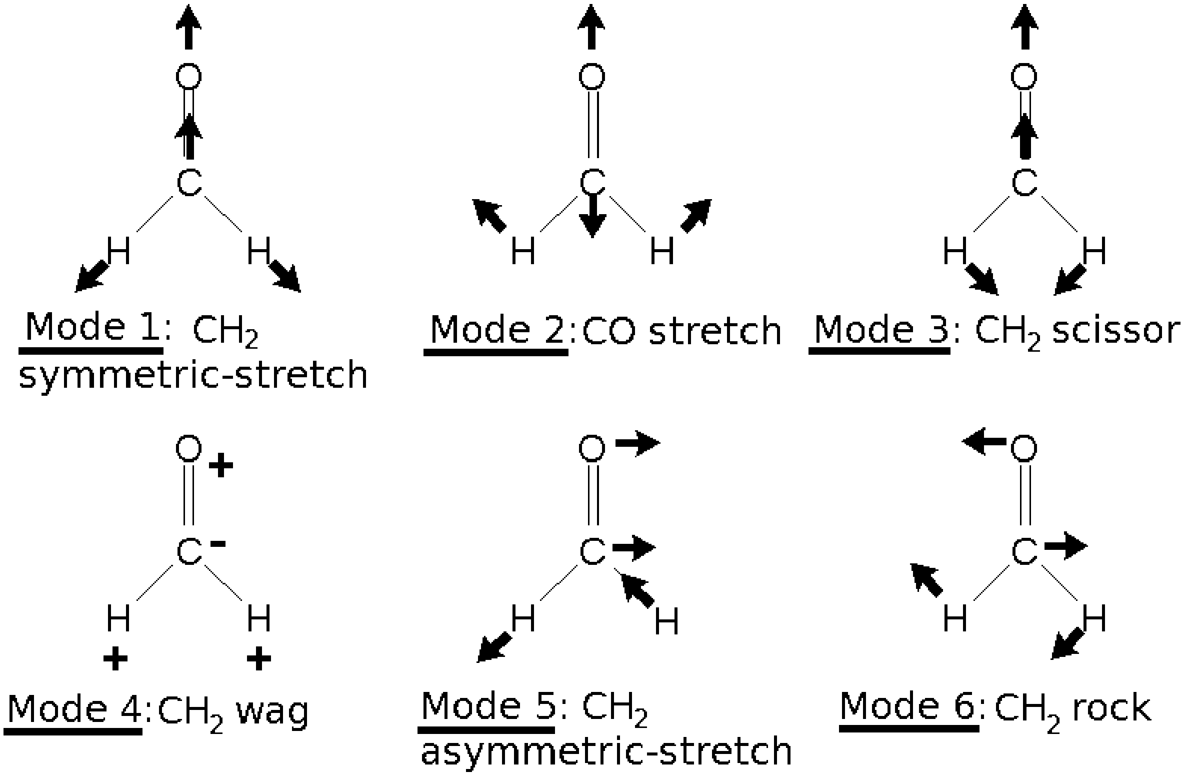

FIG. 2: The normal modes of Formaldehyde. The + and - signs in mode 4 represent movements out of the equilibrium plane.

The frequencies and reduced masses of the normal modes of the ground and excited electronic states of Formaldehyde are summarized in Table I.

TABLE I: Normal modes of Formaldehyde. Frequencies are in cm^{-1} and reduced masses in atomic mass units.

Mode	Symmetry	Ground frequency	Excited frequency	Ground reduced mass	Excited reduced mass
Mode 1	A1	2787	3120	1.0400	1.0400
Mode 2	A1	1763	1300	6.5329	1.7869
Mode 3	A1	1487	1238	1.1314	2.1101
Mode 4	B2	1154	i528	1.3493	1.3493
Mode 5	B1	2831	3254	1.1180	1.1180
Mode 6	B1	1225	832	1.3259	1.3259

The excited electronic state frequency of mode 4 is imaginary, the equilibrium structure of the molecule is not planar. The out of plane bend motion is a barrier normal mode separating the two symmetric non-planar equilibrium structures. It is especially this relatively floppy motion which invalidates the harmonic approximation for the molecule in the excited state. The computed potential energy as a function of the mode 4 coordinate, keeping all other modes in their equilibrium position is shown in Fig. 3. The line in the Figure is a fit to the numerical data using the following polynomial:

$$V(q_4) = -5.79\times10^{-5}q_4^{10}+6.98\times10^{-4}q_4^{8}-3.69\times10^{-3}q_4^{6}+1.35\times10^{-2}q_4^{4}-1.027\times10^{-2}q_4^{2}, \quad (2.1)$$

which gives the potential energy in atomic units. The difference between the fit and the numerical data is smaller than the width of the line shown in the Figure.

One also observes that the reduced masses for modes 2 and 3 (see Table I) differ in the ground and excited electronic states. The reason is that these two modes have Dushinsky [30] rotations. The transformation relating the two non mass weighted modes in the ground and excited electronic states, has been derived by using the vibrational normal mode vectors for the ground and excited electronic states, each representing the transformation from non mass weighted normal mode coordinates for the ground and excited electronic states, respectively, to the equilibrium Cartesian coordinates (which slightly differ for the ground and excited electronic states). Calling the mass weighted coordinates for the ground electronic state $q'_{i,g}, i = 2, 3$ and for the excited electronic state $q'_{i,e}, i = 2, 3$, where $q' = \sqrt{m}q$, the

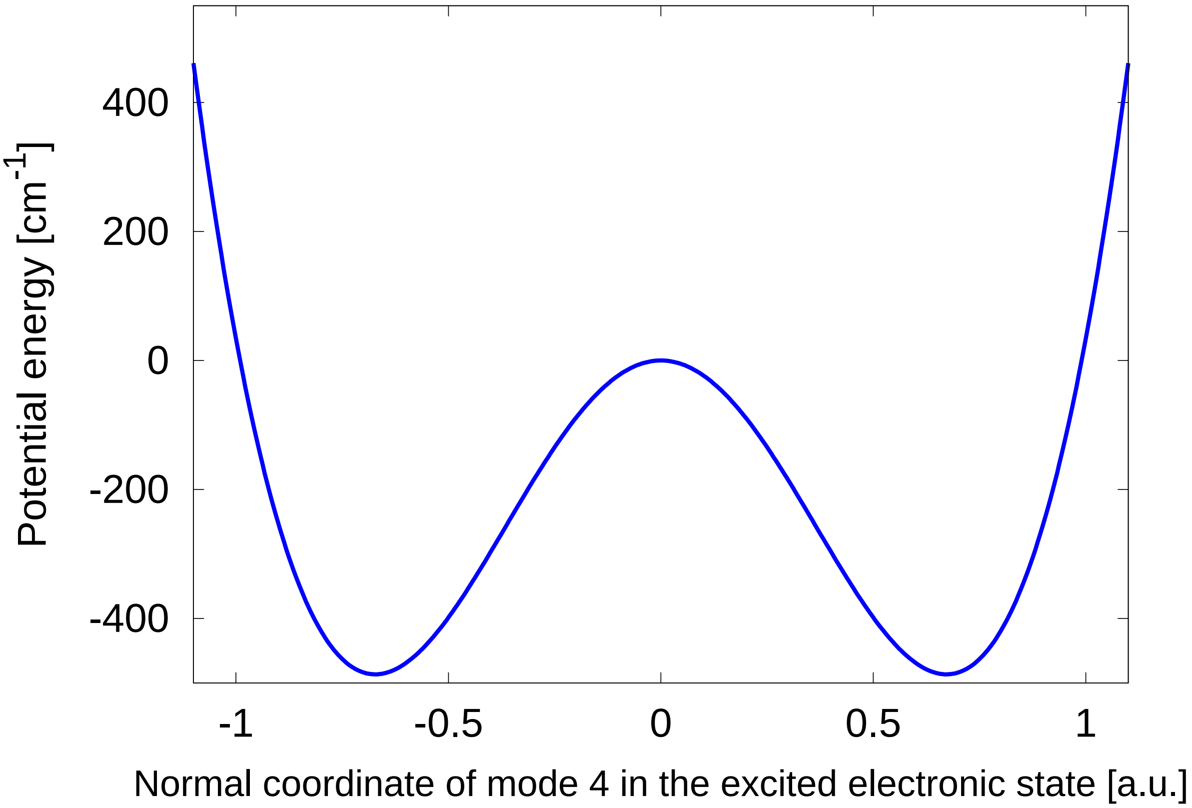

FIG. 3: The computed potential energy as a function of the normal mode coordinate q_4 for the excited electronic state of Formaldehyde.

transformation between the two non mass weighted coordinates is found to be

$$\begin{pmatrix} q'_{2,e}/\sqrt{1.7869} \\ q'_{3,e}/\sqrt{2.1101} \end{pmatrix} = \begin{pmatrix} 1.61121 & -0.42744 \\ 0.94696 & 0.61681 \end{pmatrix} \begin{pmatrix} q'_{2,g}/\sqrt{6.5329} + 0.195201 \\ q'_{3,g}/\sqrt{1.1314} + 0.02926 \end{pmatrix}, \tag{2.2}$$

where the shifts are in atomic units. Equivalently, the orthogonal transformation between the mass weighted coordinates is

$$\begin{pmatrix} q'_{2,e} \\ q'_{3,e} \end{pmatrix} = \begin{pmatrix} \cos(32.594^o) & -\sin(32.594^o) \\ \sin(32.594^o) & \cos(32.594^o) \end{pmatrix} \begin{pmatrix} q'_{2,g} \\ q'_{3,g} \end{pmatrix} + \begin{pmatrix} 0.404 \\ 0.337 \end{pmatrix}, \tag{2.3}$$

The differences in the equilibrium positions for the remaining normal modes in the ground and excited electronic states have negligible projections on the other normal modes, so that for all other modes:

$$q_{n,g} = q_{n,e} \quad \text{for} \quad n \neq 2, 3. \tag{2.4}$$

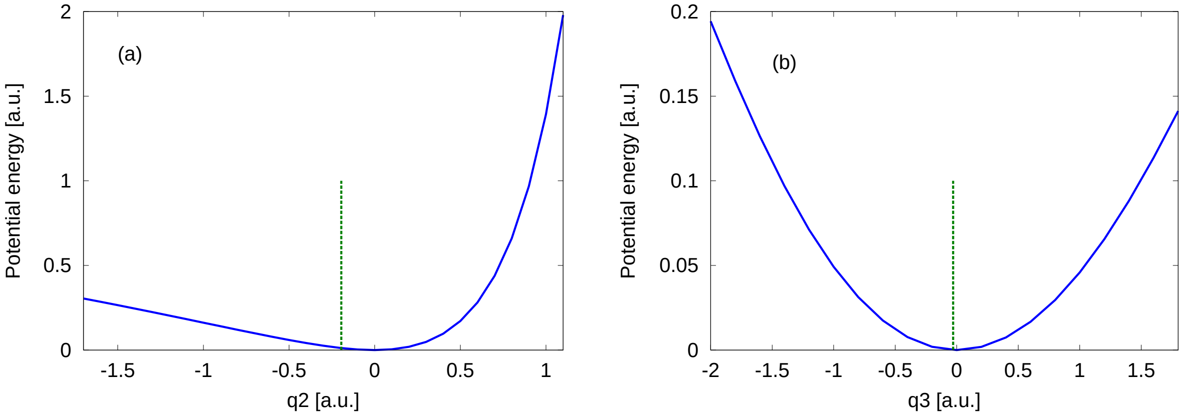

FIG. 4: The potential around the equilibrium position of the ground coordinates $q_{2,g}$ and $q_{3,g}$. The vertical (green) lines show the positions on which the excited state equilibrium is shifted, i.e -0.195201 and -0.029265 for panels (a) and (b) respectively - according to Eq. 2.2.

Figure 4 shows the potential energy around the ground equilibrium position as a function of $q_{2,g}$ in panel (a), and as a function of $q_{3,g}$ in panel (b), and on each plot we marked the excited equilibrium position. We observe that on the q_2 axis, the excited electronic potential is slightly shifted toward the dissociative side, but the ground energy at the shift position is less than 3% the dissociation energy, while on the q_3 axis the excited electronic potential is very slightly shifted toward the repulsive side. In previous work [9] we found that for the case that the excited electronic potential is shifted toward the dissociative side, the anharmonic IC rates are higher than the harmonic rates. This does not seem to be the case here, we therefore may expect the harmonic rates to be on the same order of magnitude as the anharmonic, or even higher.

B. Theory of radiationless decay

We consider the decay induced by nonadiabatic coupling from an excited vibronic state of Formaldehyde, to the ground electronic state. The radiationless decay rate is given by Fermi's golden rule [3, 31]:

$$W_{i\to f} = \frac{2\pi}{\hbar} \sum_{\nu} \sum_{\nu'} P_{\nu'} |\langle \phi_\nu \langle \chi_g | H_{\mathrm{BO}} | \chi_e \rangle \psi_{\nu'} \rangle|^2 \delta(E_\nu - E_{\nu'}) \tag{2.5}$$

where $P_{\nu'}$ is the initial probability of the molecule to be in the ν' energy level of the excited state whose eigenfunction is $\chi_e \psi_{\nu'}$, where χ_e and $\psi_{\nu'}$ are the electronic and nuclear wavefunctions, respectively. The final state ν on the ground electronic surface has the energy E_ν and eigenfunction $\chi_g \phi_\nu$, where χ_g and ϕ_ν are the electronic and nuclear wavefunctions, respectively. Energy conservation is reflected through the Dirac "delta" function $\delta(E_\nu - E_{\nu'})$.

H_{BO} is the Born-Oppenheimer coupling operator due to the breakdown of the adiabatic approximation and is expressed by a sum of nuclear momenta operating on the nuclear and electronic wave functions as follows [3, 6, 31, 32]:

$$H_{\mathrm{BO}}|\psi\chi\rangle = \sum_l \frac{1}{m_l} \left(-i\hbar\, \partial/\partial q_l |\psi\rangle\right) \left(-i\hbar\, \partial/\partial q_l |\chi\rangle\right) \tag{2.6}$$

where the sum is over all six degrees of freedom of Formaldehyde. We may hence express the matrix element coupling the excited and ground vibronic states as:

$$\langle \phi_\nu \langle \chi_g | H_{\mathrm{BO}} | \chi_e \rangle \psi_{\nu'} \rangle = -\hbar^2 \sum_l \frac{1}{m_l} \langle \phi_\nu | R_l\, \partial/\partial q_l | \psi_{\nu'} \rangle \tag{2.7}$$

with

$$R_l \equiv \langle \chi_g | \partial/\partial q_l | \chi_e \rangle, \tag{2.8}$$

representing the derivatives of the electronic wave function with respect to the nuclear coordinates. R_l are termed the non adiabatic coupling matrix elements (NACME), and may be expanded in powers of the normal mode coordinates as follows:

$$R_l = R_{l0} + \sum_k a_{lk} q_k + \sum_{nm} b_{lnm} q_n q_m + \dots , \tag{2.9}$$

Because the Formaldehyde molecule has a C_{2v} symmetric equilibrium geometry, the NACME transformed to the normal coordinates vanish at the equilibrium positions, i.e. $R_{l0} = 0$. Hence we shall use the first non vanishing order, and express R_l as a linear combination of the coordinates:

$$R_l = \sum_k a_{lk} q_k, \tag{2.10}$$

where a_{lk} are the slopes at the equilibrium position. Because of the symmetries of the molecule (see Table I) the only non zero slopes are a_{45}, a_{46}, a_{54} and a_{64}, while the other slopes are of the order of magnitude of 10^{-8} a.u.. The slopes were determined by computing the dependence of the R_j's on the relevant normal mode coordinates, as shown in panels a-c

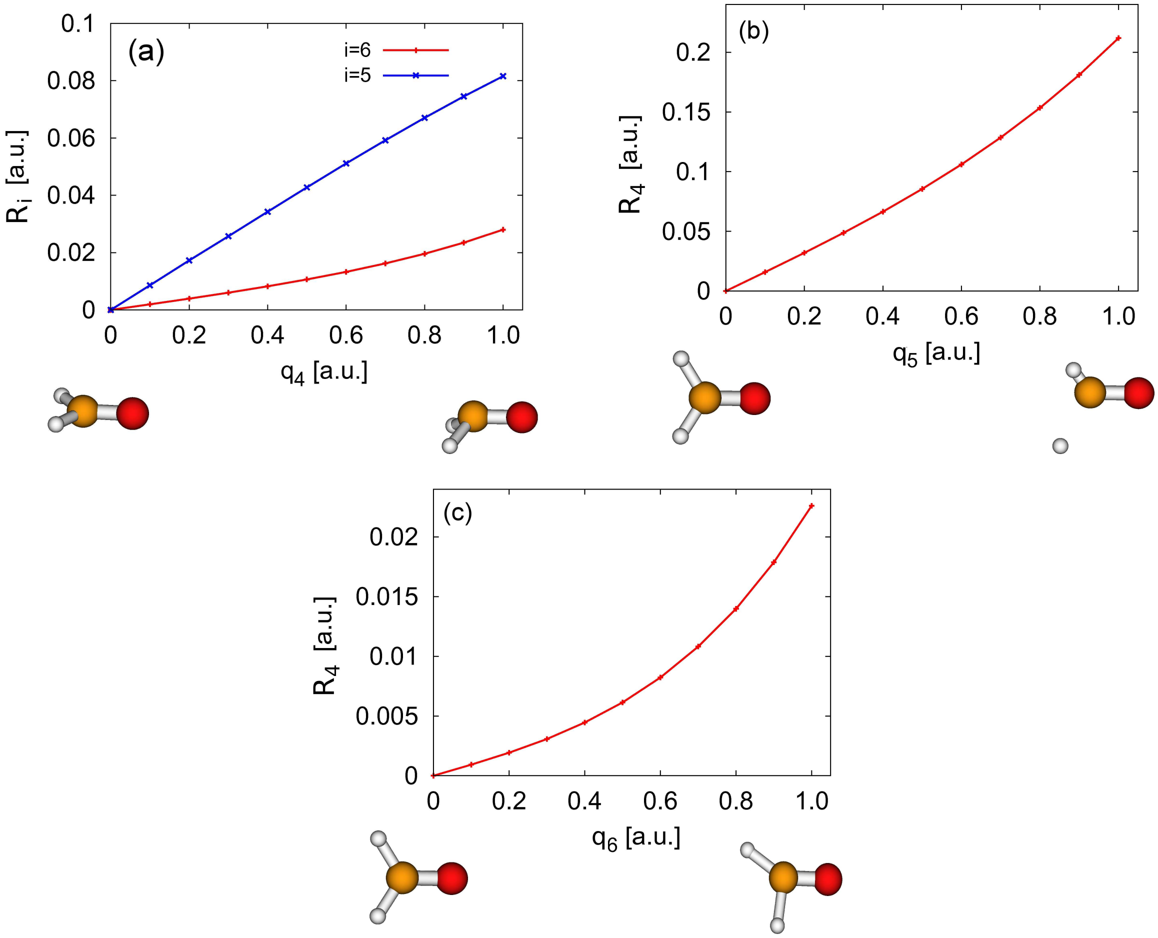

FIG. 5: The dependence of the nonadiabatic coupling elements R_j's on the relevant normal mode coordinates: panel (a) shows the dependence of R_5 and R_6 on the coordinate q_4, panel (b) shows the dependence of R_4 on the coordinate q_5 and panel (c) shows the dependence of R_4 on the normal coordinate q_6. Below each panel, the states of the molecule in the limits of $q = 0$ and $q = 1$ are depicted, for the relevant coordinate.

of Fig. 5.

The resulting matrix of non-adiabatic coupling elements used in our computations is:

$$a = \begin{pmatrix} 0 & 0 & 0 & 0 & 0 & 0 \\ 0 & 0 & 0 & 0 & 0 & 0 \\ 0 & 0 & 0 & 0 & 0 & 0 \\ 0 & 0 & 0 & 0 & 0.15 & 0.008 \\ 0 & 0 & 0 & 0.08 & 0 & 0 \\ 0 & 0 & 0 & 0.02 & 0 & 0 \end{pmatrix}, \qquad (2.11)$$

Eq. (2.5) is then rewritten as:

$$W_{i\to f} = 2\pi\hbar^3 \sum_{\nu}\sum_{\nu'} P_{\nu'} \left| \sum_{l,j} \frac{a_{lj}}{m_l} \langle \phi_\nu | q_j \partial\psi_{\nu'}/\partial q_l \rangle \right|^2 \delta(E_\nu - E_{\nu'}) \tag{2.12}$$

Using the Fourier representation of the Dirac "delta" function

$$\delta(E_\nu - E) = \frac{1}{2\pi\hbar} \int_{-\infty}^{\infty} dt\ e^{-\frac{i}{\hbar}(E_\nu - E)t} \tag{2.13}$$

one defines a time dependent density as:

$$\rho(t) \equiv \hbar^2 \sum_{l,j}\sum_{m,k} \frac{a_{lj}a_{mk}}{m_l m_m} \langle q_k \partial\psi/\partial q_m | e^{-\frac{i}{\hbar}H_g t} | q_j \partial\psi/\partial q_l \rangle \tag{2.14}$$

where H_g is the Formaldehyde electronic ground state Hamiltonian. The transition rate for a specified initial state in the excited state potential is then the Fourier transform of the density

$$W_{i\to f}(E) = \int_{-\infty}^{\infty} dt\ e^{\frac{i}{\hbar}Et} \rho(t) \tag{2.15}$$

evaluated at the energy E which is the difference between the energy of the initial vibronic excited state and the bottom of the ground electronic state potential energy surface. It is convenient to write the energy E as

$$E = \Delta E + E_i, \tag{2.16}$$

where E_i (initial energy) is the difference between the energy of the initial vibronic excited state and the barrier level of the excited electronic state potential energy surface (defined as 0 energy in Figure 3) and ΔE (the gap) is the energy difference between the above barrier level of the excited electronic state potential and the bottom of the ground electronic state potential energy surface.

The energy E_i is calculated as follows. In the excited electronic state, the system is prepared at low energies where a harmonic approximation for the motion is reasonable, except for mode 1, where as shown in Figure 3 such an approximation is not valid. We assume that the motion in the excited state is separable so that the energy E_i of the initial vibronic state, described by quantum numbers $n_1, ...n_6$ for the six modes is:

$$E_i = E_1(n_1) + \sum_{k=2}^{6} \hbar\omega_{e\,k}(n_k + 1/2) \tag{2.17}$$

where $\omega_{e,k}$ are the excited electronic state frequencies of the harmonic modes (see Table I) and $E_1(n_1)$ are the energy levels of mode 1, for excitation n_1, which have been calculated numerically. The lowest states are found at -181, -69, 410, 857, 1402, 2010 cm^{-1} where the zero of energy is the barrier (planar) top of the potential along this mode.

The gap ΔE is obtained ab-initio using DFT with the b-p functional [29], with basis functions def2-TZVP [27]. Our SCF convergence criterion was 10^{-9}, and our grid was “m5” and we used a TDDFT calculation of singlet excited states (rpas) and optimized using “egrad”. We obtained $\Delta E = 0.13039325$ a.u. $= 28,618$ cm^{-1}. From this value one may calculate ΔE_{00} defined as the energy difference between the 0’th vibronic states in the excited and ground electronic states, by adding the lowest value of E_i (which is 4685 cm^{-1}) and subtracting the lowest vibronic ground state energy obtained with a harmonic approximation which comes out to 5623.5 cm^{-1} (see Table I). The resulting calculated $\Delta E_{00} = 27679.5$ cm^{-1} underestimates the experimental result of 28188 cm^{-1} [20, 21] by 508.5 cm^{-1}.

The Hamiltonian of the ground electronic state is taken to be:

$$H_g = V(Q_1, ..Q_{12}) + \sum_{k=1}^{12} \frac{P_k^2}{2M_k} \tag{2.18}$$

where the 12 coordinates Q and 12 momenta P are the x, y and z components of the coordinates and momenta of the 4 atoms of Formaldehyde. Ordering them as C,O,H,H,we have that Q_1, Q_2 and Q_3 are the x, y and z coordinates of the C atom, Q_4, Q_5 and Q_6 are the x, y and z coordinates of the O atom, and so on. The masses M_k are the real masses of the atoms, with the same ordering $M_1 = M_2 = M_3 = 12.0107$u is the mass of the Carbon atom, $M_4 = M_5 = M_6 = 15.9994$u is the mass of the Oxygen atom, and so on. The potential energy $V(Q_1, ..Q_{12})$ is computed on the fly using the TURBOMOLE software with DFT using the b3-lyp functional [23–26].

One of the objects of the present study is to assess the validity of the harmonic approximations to the ground state electronic dynamics. For this purpose we define the harmonic ground electronic state Hamiltonian:

$$H_{g\,(\text{harmonic})} = \sum_{k=1}^{6} \frac{1}{2} m_k \omega_k^2 q_k^2 + \frac{p_k^2}{2m_k}, \tag{2.19}$$

where the sum is over all the normal modes described in Table I, q_k and p_k are the normal coordinates and momenta, and ω_k and m_k are the ground electronic state frequencies and masses given in Table I.

C. The semiclassical Herman-Kluk propagator

The Herman Kluk SCIVR propagator for a system with N degrees of freedom is [15]

$$\hat{K}_0(t) = \int_{-\infty}^{\infty} \frac{d\mathbf{p}d\mathbf{q}}{(2\pi\hbar)^N} R(\mathbf{p},\mathbf{q},t) \exp\left(\frac{i}{\hbar} S(\mathbf{p},\mathbf{q},t)\right) \; |g(\mathbf{p},\mathbf{q},t)\rangle\langle g(\mathbf{p},\mathbf{q},0)| \tag{2.20}$$

where $\mathbf{p}$ and $\mathbf{q}$ are the N dimensional momentum and coordinate variables respectively. The Herman Kluk prefactor is defined as:

$$R(\mathbf{p},\mathbf{q},t) = \sqrt{\det\left[\frac{1}{2}\left(\mathbf{\Gamma}^{1/2}\mathbf{M}_{qq}\mathbf{\Gamma}^{-1/2} + \mathbf{\Gamma}^{-1/2}\mathbf{M}_{pp}\mathbf{\Gamma}^{1/2} - i\hbar\mathbf{\Gamma}^{1/2}\mathbf{M}_{qp}\mathbf{\Gamma}^{1/2} + \frac{i}{\hbar}\mathbf{\Gamma}^{-1/2}\mathbf{M}_{pq}\mathbf{\Gamma}^{-1/2}\right)\right]}. \tag{2.21}$$

The monodromy matrices are defined by:

$$\mathbf{M}_{ab} \equiv \frac{\partial \mathbf{a}_t(\mathbf{p},\mathbf{q})}{\partial \mathbf{b}} \tag{2.22}$$

where $\mathbf{a}$ and $\mathbf{b}$ may be either $\mathbf{p}$ or $\mathbf{q}$, and $\mathbf{\Gamma}$ is a constant in time $N \times N$ matrix (usually taken to be diagonal), establishing the width of the coherent states - see Eq. (2.24). Each initial phase space point $\mathbf{p}, \mathbf{q}$ is evolved classically reaching the point $\mathbf{p}_t, \mathbf{q}_t$ at time t. The classical action along the trajectory is

$$S(\mathbf{p},\mathbf{q},t) = \int_0^t dt' \left(\mathbf{p}_t' \dot{\mathbf{q}}_t' - H(\mathbf{p},\mathbf{q})\right) \tag{2.23}$$

and the coordinate representation of the coherent state $|g\rangle$ is given by

$$\langle \mathbf{x}|g(\mathbf{p},\mathbf{q},t)\rangle = \left(\frac{\det(\Gamma)}{\pi^N}\right)^{1/4} \exp\left[-\frac{1}{2}(\mathbf{q}_t-\mathbf{x})^{\mathrm{T}}\boldsymbol{\Gamma}(\mathbf{q}_t-\mathbf{x})+\frac{i}{\hbar}\mathbf{p_t}\cdot(\mathbf{x}-\mathbf{q}_t)\right]. \tag{2.24}$$

The HK propagator as defined in Eq. (2.20) is the zero-th order approximation to the exact quantum propagator $\exp\left(-\frac{i}{\hbar}Ht\right)$. As has been shown in Refs. [33, 34] higher order corrections to the propagator may be calculated. However, the first order correction requires the a priori knowledge of the global potential surface (see Eq. 2.18), and so is not readily amenable to "on the fly" computation. Moreover, in a previous study of some model systems [9] we found that the zero-th order is an excellent approximation for the quantum propagator for internal conversion calculations. We therefore limited ourselves to using the zero-th order HK approximation given in Eq. 2.20 for computing the time dependent density function (Eq. 2.14).

Using the HK SCIVR approximation for the propagator (Eq. 2.20), the expression for the time dependent density (Eq. 2.14) becomes

$$\rho(t) = \int_{-\infty}^{\infty} \frac{d\mathbf{p}d\mathbf{q}}{(2\pi\hbar)^6} R(\mathbf{p},\mathbf{q},t)\exp\left(\frac{i}{\hbar}S(\mathbf{p},\mathbf{q},t)\right)\hbar^2\, Z(t)Z^*(0), \tag{2.25}$$

where $Z(t)$ denotes the time evolving function

$$Z(t) = \sum_{m,k}\frac{a_{mk}}{m_m}\langle q_k\partial\psi/\partial q_m|g(\mathbf{p},\mathbf{q},t)\rangle. \tag{2.26}$$

We remark that in the above sum we have 4 terms, i.e. the indices (m,k) are $(4,5)$, $(4,6)$, $(5,4)$ or $(6,4)$, according to Eq. 2.11. Each term is a multiplication of overlaps of the type $\langle q_k\psi_k|g_k(\mathbf{p},\mathbf{q},t)\rangle$, $\langle\psi_k|g_k(\mathbf{p},\mathbf{q},t)\rangle$ or $\langle\partial\psi_k/\partial q_k|g_k(\mathbf{p},\mathbf{q},t)\rangle$, k being one normal mode coordinate, except for coordinates 2 and 3 which have Dushinsky [30] rotations and must be calculated together as $\langle\psi_{2,3}|g_{2,3}(\mathbf{p},\mathbf{q},t)\rangle$.

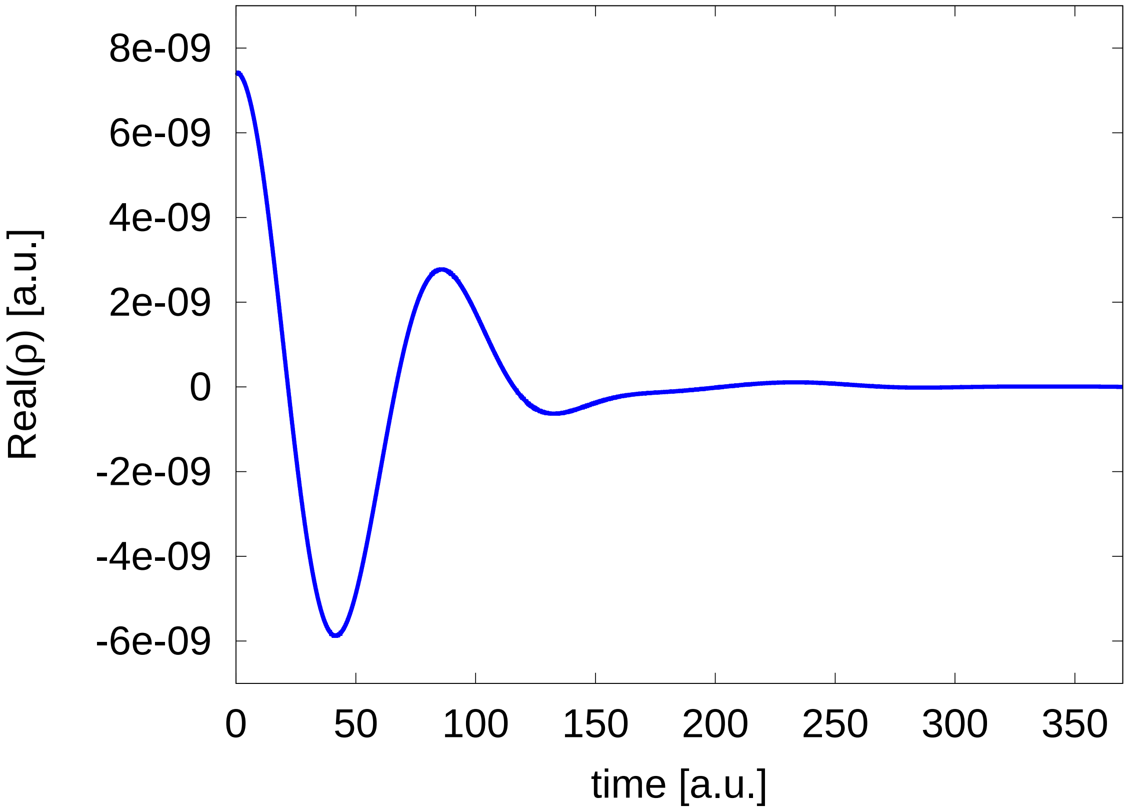

FIG. 6: The real part of the time dependent density function given in Eq. 2.14 for the decay of the ground vibrational state 00 in the excited state, calculated on the fly.

III. NUMERICAL CALCULATIONS

A. The semiclassical implementation

The time dependent density function ρ computed on the fly for the vibrational ground state function in the excited state is shown in Figure 6. Note that it decays to zero within 400 a.u., that is within 10 fsec (which is about half the average period associated with the ground electronic state frequencies). We then used this time period in all the remaining computations, using 800 time steps for the integration of the equations of motion.

The integration variables in Eq. 2.20, are the ground mass weighted normal mode coordinates and momenta, hence there are 12 integration variables. During the propagation, these coordinates and momenta are transformed to Cartesian coordinates and momenta and the propagation of the classical equations of motion is carried out using the Cartesian Hamiltonian as given in Eq. 2.18. At each point along the trajectory, the Cartesian coordinates and momenta are transformed into mass weighted normal mode coordinates and momenta and used in the calculations of the prefactor and action in Eq. 2.21 and 2.23. Similarly, the Hessians needed for the time evolution of the monodromy matrices (Eq. 2.22) and the HK prefactor have been obtained ab-initio and transformed to mass weighted normal coordinates. Because the computation of the Hessians is time consuming, only the first Hessian on each trajectory has been calculated, and the following Hessians are interpolated by a Hessian update scheme [37]. This method is valid since the Hessians change rather smoothly along the trajectories. Comparison of the results of the Hessian update scheme with the numerically exact Hessians along a single trajectory shows that the update scheme leads to a typical error of 5%, which we believe is acceptable. The expense of computing the Hessians numerically exactly along the trajectory would have made the computation too expensive for us to carry out.

The width matrix $\mathbf{\Gamma}$ appearing in the coherent states was taken to be diagonal in the normal mode representation with elements $\Gamma_{jj} = m_j \omega_j / \hbar$, where $m_j = 1$ when using the mass weighted coordinates and momenta and the ω_j are the ground electronic state harmonic frequencies as given Table I. In the computation of the overlap between the coherent states in the ground state representation and the initial states in the excited state, the transformation between the two sets of the coordinates, including Dushinsky rotation and shifts have been incorporated. The phase space integrals needed to obtain the time dependent density were performed using a Monte Carlo integration. The weight function used was obtained from the overlap of the coherent states with the initial wavefunction of the excited state, according to Eq.2.26. Convergence was achieved using 60000 trajectories leading to an accuracy of about 1.5%. This has been measured by comparing the standard deviation of the difference between the density functions resulting from the whole sample of 60000 trajectories and from half of the above sample.

B. Results

We calculated the life times (i.e. $1/W_{i \to f}$ in Eq.2.15) for several initial excited states, with the ab-initio potential as defined through Eq. 2.18 and with the harmonic approximation according to Eq. 2.19. The results, plotted in Figure 7 are tabulated in Table II, which also provides the experimental results reported in Ref. [36].

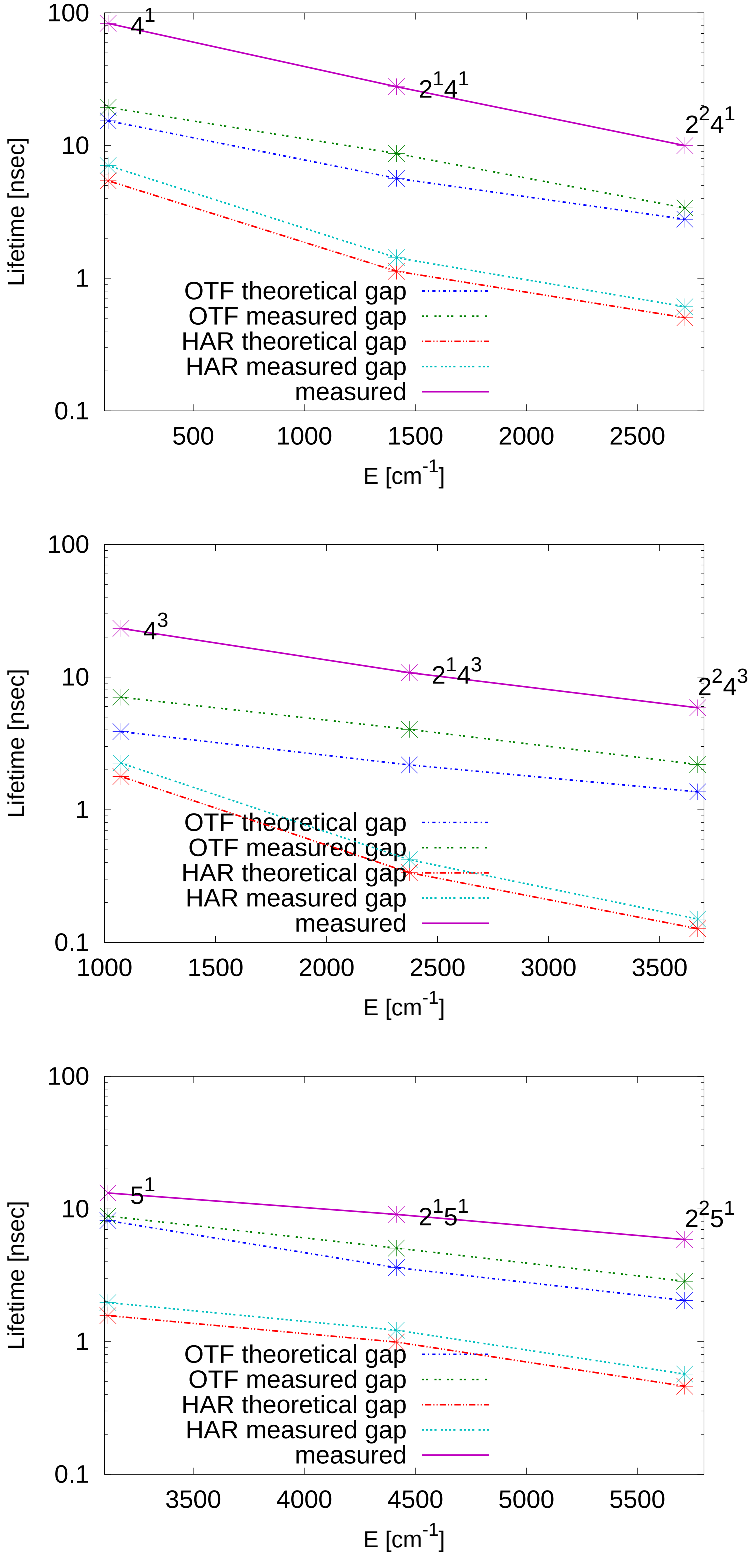

FIG. 7: The lifetimes for the group of states 4^1 in panel (a), 4^3 in panel (b) and 5^1 in panel (c). The states are named so that the regular script number represents the number of the mode (shown in Figure 2) and the superscript number is the excitation level. In each panel we show results for the on-the-fly (OTF) ab-initio computation using either the theoretical or the measured gap, results for the harmonic computation (HAR) using either the theoretical or the measured gap and the experimentally measured results, shown in Table II in the third, fourth and fifth columns, respectively.

TABLE II: Internal conversion lifetimes [nsec] for different initial excited states. The results correspond to the ab-initio (anharmonic) potential, the harmonic potential and the experimental results reported in Ref. [36]. The 2 columns separated by a comma in the ab-initio and harmonic columns represent 2 variants of the results: the left result obtained by using the ab-initio gap ΔE from Eq.2.16 and the right result obtained by using the experimental gap from Ref. [21], which is larger by 508.5 cm^{-1} than the ab-initio gap. The energies of the states are given in cm^{-1} and are relative to the ground (00) vibrational state in the excited electronic state.

State	Energy	Ab-initio potential	Harmonic potential	Measured
4^1	117	15.4 , 19.4	5.43 , 7.07	83.3
$2^1 4^1$	1415	5.67 , 8.71	1.13 , 1.43	27.8
$2^2 4^1$	2714	2.78 , 3.39	0.504 , 0.61	10.0
4^3	1074	3.88 , 7.04	1.78 , 2.25	23.3
$2^1 4^3$	2373	2.18 , 4.03	0.336 , 0.42	10.8
$2^2 4^3$	3672	1.37 , 2.19	0.127 , 0.15	5.88
5^1	3116	8.16 , 8.84	1.57 , 1.97	13.2
$2^1 5^1$	4414	3.61 , 5.07	0.992 , 1.22	9.09
$2^2 5^1$	5713	2.04 , 2.85	0.461 , 0.57	5.88

One observes that the lifetimes obtained using the anharmonic ab-initio potential with the theoretical energy gap, are around 5 times smaller than the experimental lifetimes from Ref. [36] for the 4^1 and 4^3 groups and around 2.3 times smaller for the 5^1 group. However, the ab-initio lifetimes get closer to the experimental results when using the measured energy gap between excited and ground electronic states.

We also remark that the lifetimes obtained with the harmonic approximation potential are farther from the experimental results than those obtained by the ab-initio potential.

One possible reason for the discrepancy between the ab-initio results and experiment is that the ab-initio estimates of the non-adiabatic coupling matrix elements (NACME), see Figure 5 and Eq. 2.11, are not sufficiently accurate. The ab-initio decay rates are quadratic with respect to the NACME slopes in Eq. 2.11 (see Eq.2.14). If one multiplies the computed NACME by a factor of 1/1.65 one obtains much better agreement with experiment, as seen in Figure 8. The scaled results differ from the measured results by 17% for the 4^1 and 4^3 groups, and approximately 30% for the 5^1 group.

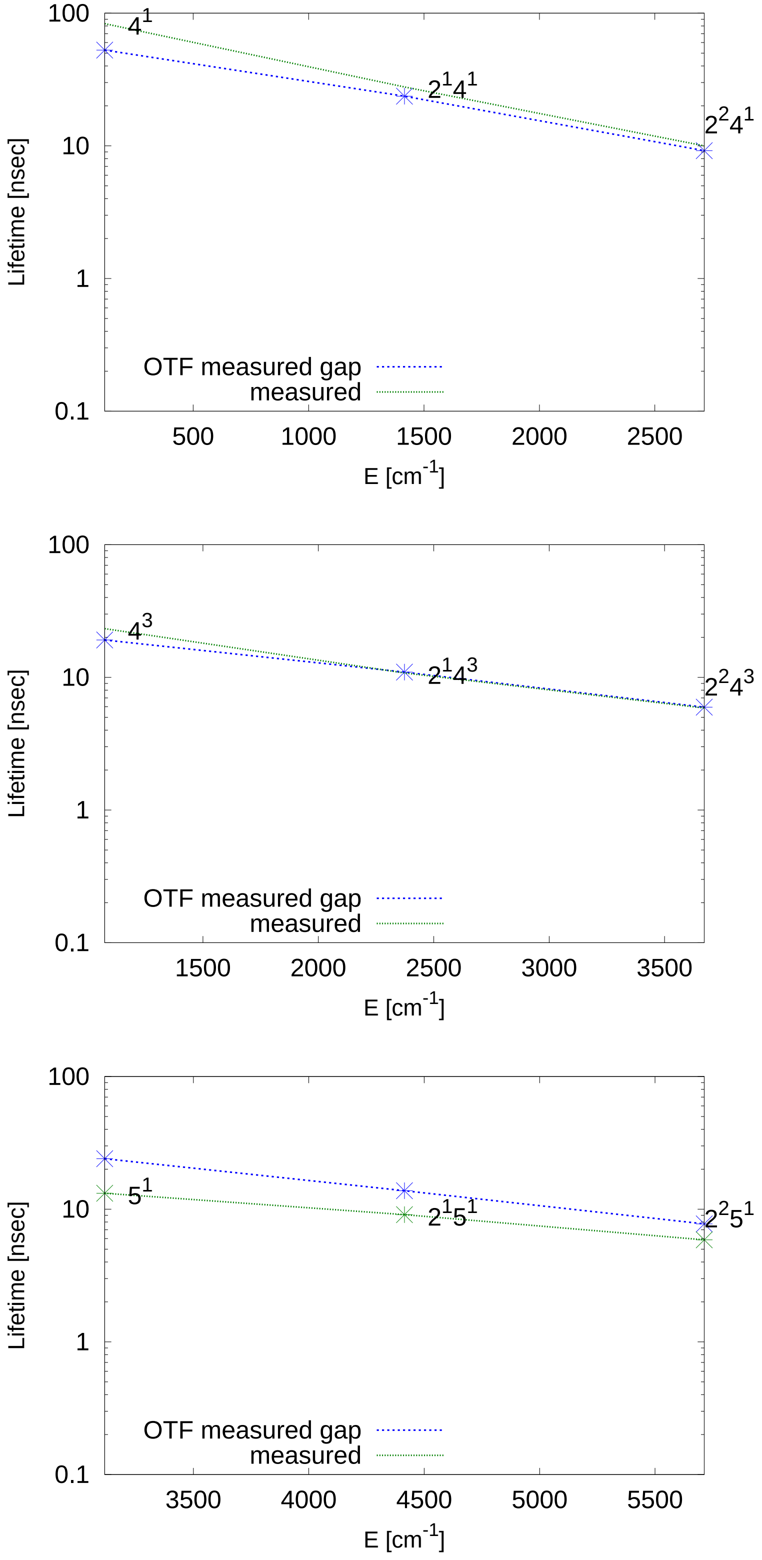

FIG. 8: Lifetimes comparisons between measured results and the ab-initio on the fly computation obtained after dividing the NACME slopes by 1.65. The group of states 4^1, 4^3 and 5^1 are shown in panels (a), (b) and (c), respectively.

IV. CONCLUDING REMARKS

We calculated the internal conversion rate for the excited states of CH_2O, using the HK SCIVR method and on-the-fly molecular dynamics. We used Fermi's golden rule to calculate the internal conversion rate, and expressed this rate as a Fourier transform of an overlap function, which has been evaluated using the HK SCIVR approximation. The molecule parameters were evaluated with TURBOMOLE, and used in the HK SCIVR calculation. TURBOMOLE was also used to calculate the potential energy for the classical trajectories used in the HK SCIVR calculation.

The initial vibronic states on the excited electronic state were computed approximately, using a separable approximation. This does not seriously affect the computed decay rates, since the change in energy which would be obtained from a more precise computation would create only a minor relative change of the energy in the ground state which would not suffice to account for the discrepancy in the magnitude of the theoretical and experimental decay rates.

From the comparison with experiment, we may reach a number of conclusions:

- A harmonic approximation for the dynamics is insufficient. There is a rather large difference between IC lifetimes computed with the harmonic and SCIVR approximations.
- The first principles based computation of the force field is not sufficiently accurate for reproducing the measured results reported in Ref. [36]. The calculated energy gap between the two electronic states is not accurate enough.
- The first principles based dynamics computation using the SCIVR approximation reproduces rather accurately the relative effects of initiating the internal conversion from different vibronic states of Formaldehyde.
- Good agreement with experiment was achieved by scaling the NACME by a single parameter and using the measured energy gap. This indicates that most likely the main difficulty is in the accurate computation of electronic properties but that the nuclear force field is sufficiently accurate.
-

At the end of the day, the Formaldehyde molecule is sufficiently small that one could create a fitted force field for the molecule and then compute the internal conversion rates quantum mechanically, using the MCTDH methodology. With present day computational resources, there is no need to use an SCIVR approximation for this specific system. However, the computation presented here, demonstrates that the SCIVR methodology is robust and can be used for the computation of molecular internal conversion rates. A limitation in applying the methodology to larger systems is that the numerical expense for the dynamics scales at least as the number of degrees of freedom squared. Given reasonable computational resources, this implies that it may be possible to use the SCIVR on the fly methodology for molecules with up to 20 atoms.

Acknowledgments

This work has been supported by grants from the Israel Science Foundation and the German-Israeli Foundation for Scientific Research and Development.

---

[1] N.J. Turro, Modern molecular photochemistry, *Benjamin Cummings, Menlo Park, CA* (1978)

[2] S.H. Lin, J. Chem. Phys. **47**, 3759 (1966).

[3] S.H. Lin and R. Bersohn, J. Chem. Phys. **48**, 2732 (1968).

[4] S.H. Lin, C.H. Chang, K.K. Liang, R. Chang, J.M. Zhang, T.-S. Yang, M. Hayashi, Y.J. Shiu, and F.C. Hsu, Adv. Chem. Phys. **121**, 1 (2002).

[5] M. Etinski, J. Tatchen and C.M. Marian, J. Chem. Phys. **144**, 154105 (2011).

[6] E. S. Yeung and C. B. Moore, J. Chem. Phys., **60**, 2139 (1974).

[7] H. Wang, C. Zhu, j.-G. Yu and S.H. Lin, J. Phys. Chem. A **113**, 14407 (2009).

[8] R. He, L. Yang, C. Zhu, M. Yamaki, Y.-P. Lee and S.H. Lin, J. Chem. Phys. **134**, 094313 (2011).

[9] R. Ianconescu, E. Pollak, J. Chem. Phys. 134(23), 234305 (2011).

[10] Q. Peng, Y.P. Yi, Z.G. Shuai and J. Shao, J. Am. Chem. Soc. **129**, 9333 (2007).

[11] Q. Peng, Y. Niu, C. Deng and Z. Shuai, Chem. Phys. **370**, 215 (2010).

[12] For recent reviews and applications see the book ”Multidimensional Quantum Dynamics: MCTDH Theory and Applications” edited by H.-D. Meyer, F. Gatti, and G. A. Worth (Wiley VCH, 2009).

[13] T. Nakajima, S. Kato, J. Chem. Phys. 105 (14), (1996)

[14] W.H. Miller, J. Phys. Chem. A **105**, 2942 (2001).

[15] M. F. Herman and E. Kluk, J. Chem. Phys. **91**, 27 (1984).

[16] M. Ceotto, S. Atahan, S. Shim, G.F. Tantardini, and A. Aspuru-Guzik, Phys. Chem. Chem. Phys. **11**, 3861 (2009).

[17] M. Ceotto, S. Atahan, G.F. Tantardini, and A. Aspuru-Guzik, J. Chem. Phys. **130**, 234113 (2009).

[18] M. Ceotto, S. Valleau, G.F. Tantardini, and A. Aspuru-Guzik, J. Chem. Phys. **134**, 234103 (2011).

[19] M. Ceotto, G.F. Tantardini, and A. Aspuru-Guzik, J. Chem. Phys. **135**, 214108 (2011).

[20] J. Tatchen, E. Pollak, J. Chem. Phys. **130**, 041103 (2009).

[21] S. J. Strickler and R. Barnhart, J. Phys. Chem. **86**, 448, (1982)

[22] R. Ahlrichs, M. Bär, H.P. Baron, R. Bauernschmitt, S. Böcker,N. Crawford, P. Deglmann, M. Ehrig, K. Eichkorn, S. Elliott, F. Furche, F. Haase, M. Häser, C. Hättig, A. Hellweg, H. Horn, C. Huber, U. Huniar, M. Kattannek, A. Köhn, C. Kölmel, M. Kollwitz, K. May, P. Nava, C. Ochsenfeld, H. Öhm, H. Patzelt, D. Rappoport, O. Rubner, A. Schäfer, U. Schneider, M. Sierka, O. Treutler, B. Unterreiner, M. von Arnim, F. Weigend, P. Weis, and H. Weiss, TURBOMOLE, version 5.10, Universität Karlsruhe, 2008.

[23] A.D. Becke, J.Chem.Phys. **98** 5648-5652, (1993)

[24] C. Lee, W. Yang, R.G. Parr, Phys. Rev. B **37**, 785-789, (1988)

[25] S.H. Vosko, L. Wilk, M. Nusair, Can. J. Phys. **58**, 1200-1211, (1980)

[26] P.J. Stephens, F.J. Devlin, C.F. Chabalowski, M.J. Frisch, J.Phys.Chem. **98**, 11623-11627, (1994)

[27] D. Rappoport and F. Furche, J. Chem. Phys. **133**, 134105 (2010).

[28] K. Eichkorn; F. Weigend; O. Treutler; R. Ahlrichs, Theor. Chem. Acc., **97(1-4)**, 119-124, (1997).

[29] R. Bauernschmitt, R. Ahlrichs, Chem. Phys. Lett., 256(4-5), 454-464, (1996).

[30] F. Dushinsky, Acta Physicochim. URSS 7, 551 (1937).

[31] Q. Peng, Y.P. Yi, Z.G. Shuai and J. Shao, J. Chem. Phys. **126**, 114302 (2007).

[32] S. Fischer, J. Chem. Phys. **53**, 3195 (1970).

[33] S. Zhang and E. Pollak, Phys. Rev. Lett. **91**, 190201 (2003).

[34] S. Zhang and E. Pollak, J. Chem. Phys. **119**, 11058 (2003).

[35] E. Pollak and J. Shao, J. Phys. Chem. A **107**, 7112 (2003).

[36] R.G. Miller, E.K.C. Lee, Chem. Phys. Lett., 33(1), 104 (1975)

[37] M. Ceotto, Y. Zhuang, and W.L. Hase, J. Chem. Phys. **138**, 054116 (2013).